

EXAFS Debye–Waller Factor and Ligand Exchange Reaction of Hydrated Metal Complexes

Takafumi Miyanaga,* Hideto Sakane,[†] and Iwao Watanabe^{††}

Department of Physics, Faculty of Science, Hirosaki University, Hirosaki, Aomori 036

[†]Department of Applied Chemistry and Biotechnology, Faculty of Engineering, Yamanashi University, Kofu, Yamanashi 400

^{††}Department of Chemistry, Faculty of Science, Osaka University, Toyonaka, Osaka 560

(Received June 6, 1994)

The EXAFS (Extended X-Ray Absorption Fine Structure) spectra of hydrated transition metal complexes were measured to investigate the relation between the Debye–Waller factor in EXAFS, σ^2 , and their ligand exchange reaction rate constant, k_1 , in aqueous solution. A good correlation between these two factors was obtained for various transition metal ions. The relation between σ^2 and $\log k_1$ is studied theoretically using the Arrhenius theory. The introduction of an anharmonic Morse function as the interaction potential was found to lead to a simple expression connecting σ^2 and $\log k_1$, which is in accordance with the experimental results. It is also found that k_1 correlates not only with σ^2 but also a third order cumulant in EXAFS, C_3 ; the greater the k_1 value, the greater the increase in C_3 with temperature. The behavior of C_3 implies that the anharmonicity in the potential of the metal–oxygen interaction must be taken into consideration for the study of the ligand exchange reaction.

X-Ray Absorption Fine Structure (XAFS) spectroscopy is a powerful technique for investigating the local structure in solution.¹⁾ The main information which the extended XAFS (EXAFS) provides is the interatomic distance, the number of surrounding atoms, and the disorder in structure or the fluctuation in interatomic distance (the Debye–Waller factor, σ^2). σ^2 may contain information regarding the dynamical disorder in the interatomic distance in addition to the static disorder, although we have little knowledge of σ^2 in EXAFS. It should be noted here that σ^2 , as determined by the EXAFS, differs from that obtained by the diffraction technique for crystals. The Debye–Waller factor of the diffraction refers to the displacement from the crystal lattice due to thermal motion. On the other hand, that of the EXAFS refers to the disorder in the interatomic distance between a pair of atoms, the X-ray absorbing and the photoelectron scattering atoms, thus a strong correlation exists between σ of EXAFS and the phonon spectrum.²⁾

There exist some EXAFS applications to the study of chemical reactivity of metal complexes in solution. Brunschwig et al.³⁾ have collected the bond lengths and their differences between di- and tri-valent states for a number of metal complexes in solution. They obtained a correlation of the self-electron-exchange rate constant with the difference in the metal–ligand bond distance between two oxidation states in accord with the Marcus–Hush theory. Sham^{4,5)} was the first to point out

that the ligand exchange rate constant, k_1 , in aqueous solution of 3d hydrated metal ions (Cr^{2+} , Cr^{3+} , Mn^{2+} , Fe^{2+} , Fe^{3+} , Co^{2+} , Ni^{2+} , and Cu^{2+}) should be closely related to its EXAFS σ value. He suggested that the large σ values of axial oxygen atoms of Cu^{2+} and Cr^{2+} hydrated complexes in aqueous solution arise from fast water exchange at their axial sites. Recently, it has been reported⁶⁾ that the water exchange rate correlates with the EXAFS oscillation amplitude not only for solutions but also for solid-phase samples. This means that the σ value is not affected by the real exchange motion of the ligand water molecule but reflects the strength or stiffness, of the atom–atom interaction. More recently, it was suggested that a good correlation exist between the third order cumulant, C_3 , in the EXAFS formula and k_1 .⁷⁾

It is apparent that the higher order cumulants must be included in the EXAFS formula when the anharmonic potential effect is significant.^{8–10)} The EXAFS spectroscopy is sensitive to the anharmonic potential effects and its temperature dependence provides unique information about anharmonic interaction. A theoretical approach to the Debye–Waller factor in EXAFS from the first principle quantum statistics was given¹¹⁾ and relations between the parameters of the anharmonic Morse potential and the cumulants in EXAFS for a one-dimensional model were presented.¹²⁾

In this paper, firstly the values of σ^2 for solution and solid-phase samples of hydrated metal complexes are

collected until the number was greater than that Sham reported, and the correlation between σ^2 and $\log k_1$ is shown schematically. Secondly, the theoretical bases of the relation between σ^2 and $\log k_1$ is predicted by combining a simple Arrhenius equation and an expression for the Debye–Waller factor developed recently.¹²⁾ Finally, the temperature dependences of σ^2 and C_3 over the temperature range of 20 K to 300 K for solid hydrated complexes are discussed.

Experimental and Data Analysis

Data Collection. All the *K*-edge absorption spectra were recorded in a transmission mode at BL 6B and BL 7C of the Photon Factory, the Institute of High Energy Physics (KEK) in Tsukuba. Si(111) double crystal monochromators were used. To reduce the higher order components in X-rays, the second crystal was detuned so that the absorbance at the edge was maximized, then the photon flux was reduced to about 50% of the original intensity. For Cr *K*-edge measurements, a quartz mirror was inserted into the X-ray beam to reduce the higher order X-rays. The storage ring was operated at 2.5 GeV and the ring current was 200–300 mA.

Solid samples of $\text{Cr}(\text{ClO}_4)_3 \cdot 6\text{H}_2\text{O}$, $\text{Fe}(\text{ClO}_4)_3 \cdot 8\text{H}_2\text{O}$, $\text{Mn}(\text{ClO}_4)_2 \cdot 8\text{H}_2\text{O}$, $\text{Ni}(\text{ClO}_4)_2 \cdot 6\text{H}_2\text{O}$, and $\text{Zn}(\text{ClO}_4)_2 \cdot 6\text{H}_2\text{O}$ were purchased from Soekawa Chemicals, Ltd. and $\text{CoSO}_4 \cdot 7\text{H}_2\text{O}$ was from Aldrich Chemical Company, Inc. The solid powdered samples were held on adhesive tapes and measurements were performed at 20, 100, 200, and 297 K in a cryostat. Since most of the perchlorate complexes are deliquescent, the samples are treated in dry nitrogen gas. The solution samples were prepared by dissolving the above salts. Perchloric or sulfuric acid was added in the solution in order to prevent the hydrolysis. The solutions of Ti^{3+} and Fe^{2+} ions were prepared by the electric reductions of titanium(IV) sulfate and iron(III) perchlorate solutions, respectively. The solution of V^{3+} ion was prepared by mixing equal amounts of V^{2+} and V^{4+} sulfate solutions. Since lower valence state ions are very sensitive to air and are easily oxidized, all procedures as well as X-ray absorption measurements were also performed under the nitrogen gas atmosphere.

The concentrations of metal ions in solution were 0.5–1.0 mol dm^{-3} . The 0.1 mol dm^{-3} Rb^+ aqueous solution was prepared by dissolving RbCl . The sample thicknesses were set to obtain appropriate edge jumps for solid and solution samples. The edge jumps for solid samples were 0.9 for Cr^{3+} , 1.1 for Fe^{3+} , 0.9 for Co^{2+} , 1.2 for Ni^{2+} , 1.3 for Mn^{2+} , and 1.9 for Zn^{2+} , and for solution samples 0.5 for Cr^{3+} (1.0 mol dm^{-3}), 1.45 for Ti^{3+} (0.75 mol dm^{-3}), 0.95 for V^{2+} (1.0 mol dm^{-3}), 0.62 for V^{3+} (1.0 mol dm^{-3}), 0.73 for Fe^{2+} (0.5 mol dm^{-3}), 0.95 for Fe^{3+} (0.5 mol dm^{-3}), 0.58 for Co^{2+} (1.0 mol dm^{-3}), 0.75 for Ni^{2+} (1.0 mol dm^{-3}), 1.7 for Mn^{2+} (1.0 mol dm^{-3}), 1.94 for Cu^{2+} (1.0 mol dm^{-3}), and 1.0 for Zn^{2+} (1.0 mol dm^{-3}). That for Rb^+ is 0.14 for 0.1 mol dm^{-3} . All solution data were obtained at room temperature (297 K).

Data Analysis. The EXAFS interference function, $\chi(k)$, was extracted from the absorption spectrum and was Fourier transformed according to a procedure described in Ref. 13.

The theoretical EXAFS function fitted to the experimen-

tal data is

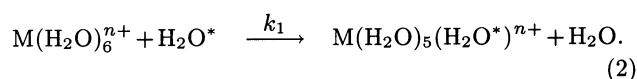
$$\chi(k) = \frac{B |f(k, r)|}{kr^2} \exp\left(-\frac{2r}{\lambda(k)}\right) \exp(-2\sigma^2 k^2) \sin[2kr + \varphi(k, r) - \frac{4}{3}C_3 k^3], \quad (1)$$

where r is the interatomic distance, and $|f(k, r)|$ and $\varphi(k, r)$ are the backscattering amplitude and the total phase shift function, respectively, which were calculated by Mckale et al.¹⁴⁾ using the curved-wave method. The k -range used for the curve-fitting is somewhere between 4 and 10 \AA^{-1} . $\lambda(k)$ is the electron mean free path being fixed as $\lambda(k) = k/0.5$ according to the typical value for inorganic materials.¹⁵⁾ As will be discussed later, it should be noted that the third order cumulant C_3 is not negligible in the present analysis. $B(=S_0^2 N)$ is a parameter consisting of the coordination number, N , and the reduction factor due to many body effects, S_0^2 . The photoelectron wavenumber k is a function of ΔE_0 as $k = \sqrt{k_0^2 - 2m\Delta E_0/\hbar^2}$, where ΔE_0 is the shift in the inner shell potential referred to the energy at the half of edge jump in the absorption spectra. In the present analyses, the non-linear least-squares curve-fitting calculations are applied to a nearest neighbor shell. ΔE_0 and B are fixed to the values determined from the spectrum taken at 20 K for each complex and they are used for the analyses for the other temperatures. The metal–oxygen distance r for solid sample is assumed to be the same as that for 20 K. This is because there exists a strong correlation between r and C_3 , thus the fitting calculations often give meaningless value for them unless r is fixed at a constant value. The r -range used for the Fourier filtering is about 1.5 \AA around the first peak. Since the lower and higher edges in the k -space spectrum are easily distorted by the Fourier filtering, they are not included in the calculation. The residual values defined in Ref. 13 are 1.5–5.0%.

The uncertainty in the Debye–Waller factor is defined as its deviation from the best-fit value when the deviation doubles the sum of squared residuals, meanwhile allowing all other variables to float.¹⁶⁾ The uncertainty, which is called “error bar” by “International Workshop on Standards and Criteria in X-Ray Absorption Spectroscopy, 1988,”¹⁶⁾ reflects all the effects of the correlations between the parameters.

Results and Discussion

Relation between σ^2 and $\log k_1$. In the crystals of perchlorate and sulfate, all the 3d transition metal complexes have an octahedral six-coordinate structure, MO_6 . In aqueous solution, they keep the octahedral MO_6 structure and the first nearest neighbor atoms are the oxygen atom of the water. The complexes exchange the ligand water molecule with the solvent water molecule in solution. The rate constant, k_1 , of the exchange reaction pertains to the following reaction,



The correlation found previously between k_1 and EXAFS oscillation amplitude for M–O interaction implies that the interaction strength governs both k_1 and the

EXAFS amplitude.⁶⁾ It is expected, then, that σ^2 for the M–O interaction also correlates with k_1 . Sham has collected the values of σ for Cr^{2+} , Cr^{3+} , Mn^{2+} , Fe^{2+} , Fe^{3+} , Co^{2+} , Ni^{2+} , and Cu^{2+} ions and pointed out the correlation of σ and k_1 , however, it has not been shown schematically. Figure 1 shows a plot of the σ^2 value against $\log k_1$; we can see a good correlation between them. For several complexes, both σ^2 values obtained for solid and solution states are plotted. The similar dependence of both data upon $\log k_1$ indicates that the σ^2 value does not reflect the real ligand exchange but rather the intrinsic character of the metal–oxygen bond.

The octahedral structures of Cr^{2+} or Cu^{2+} are distorted by the Jahn–Teller effect by which the two axial metal–oxygen bonds are elongated.^{4,5)} The σ^2 values for the axial bonds are larger than those for equatorial ones. For Cu^{2+} complex in solution, the former is 0.018 \AA^2 and the latter is 0.0048 \AA^2 . Swift and Connick¹⁸⁾ have obtained the k_1 values for the axial and equatorial sites of Cu^{2+} individually. In Fig. 1, both σ^2 and k_1 values for Cu^{2+} are those for the equatorial site.

Theoretical Treatment of the Relation between σ^2 and $\log k_1$. In the previous section, a qualitatively good correlation between σ^2 and $\log k_1$ has been obtained. In this section, we give the theoretical bases of that relation. To simplify the model, some assumptions are introduced. The anharmonic potential adapted here is that of the Morse function as

$$V(x) = D(e^{-2\alpha x} - 2e^{-\alpha x}), \quad (3)$$

where x is the relative displacement of the interatomic distance, α is the parameter for width of the potential, and D is the dissociation energy. The theoretical approach to the EXAFS Debye–Waller factor using the Morse interatomic potential of Eq. 3 leads to the following simple expression for σ^2 at a certain temperature

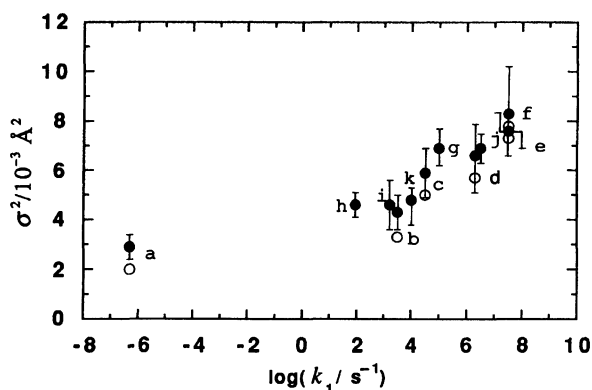


Fig. 1. Relation between σ^2 and $\log k_1$ for (a) Cr^{3+} , (b) Fe^{3+} , (c) Ni^{2+} , (d) Co^{2+} , (e) Mn^{2+} , (f) Zn^{2+} , (g) Ti^{3+} , (h) V^{3+} , (i) V^{2+} , (j) Fe^{2+} , and (k) the equatorial oxygen atom of Cu^{2+} . Open circles denote solid and closed circles solution samples. The error bars represent the uncertainties for the solution data. The k_1 values are collected from Ref. 17.

under certain condition,¹²⁾

$$\sigma^2 \propto \frac{a^2 \hbar}{8\pi\alpha\sqrt{2D}}, \quad (4)$$

where a is the lattice constant. The approximations under which Eq. 4 is derived are discussed briefly below. The theory gives a higher order expression for σ^2 beyond the harmonic approximation for a diatomic one-dimensional model. The estimated anharmonic correction by the theory is about 15% in the second order cumulant at room temperature; therefore, we neglect the anharmonic effect in σ^2 . Although the theoretical calculation is limited to the one-dimensional chain, the conclusion must be valid since the single scattering process dominates in EXAFS. However, the expression given under the harmonic approximation is still too complicated to study the relation between σ^2 and $\log k_1$ for the present metal complexes. We assume further that the optical phonon is more important than the acoustic one in molecules or in metal complexes in solution, i.e., the acoustic contribution can be neglected. According to the theory, σ^2 for the optical mode slightly varies with temperature and is almost constant at the value pertaining to the zero point vibration for the samples measured at around room temperature. The vibrational mode which affects the EXAFS most is the stretching mode for metal–oxygen interaction. The frequency is normally $400\text{--}500 \text{ cm}^{-1}$ for the hydrated 3d metal complexes thus the vibrationally excited states are neglected; the distribution of the molecules in the excited state is about 12% at room temperature for 400 cm^{-1} vibrational mode.

Next, we apply the Arrhenius theory expressed as Eq. 5 to the ligand exchange reaction in aqueous solution.

$$k_1 = A \exp(-E_a/k_B T) \\ \text{or } \log k_1 = \log A - \frac{E_a}{2.3026k_B T}, \quad (5)$$

where E_a is the activation energy and A is the frequency factor or the preexponential factor independent of the activation energy. The ligand exchange reaction of 3d metal complexes is classified as neither a dissociative nor an associative process but as an intermediate one. However, for simplicity we assume that the reaction proceeds through the dissociative process predominantly and that the Morse-type interatomic potential is operative as a reaction coordinate, thus E_a is replaced by D . Then we obtain

$$E_a = D = 2.3026k_B T(\log A - \log k_1). \quad (6)$$

This assumption means that the ligand exchange rate depends only on D . Then σ^2/a^2 is proportional to $D^{-1/2}$ if the parameter α for the metal ions used is assumed to be a constant. Finally, we obtain a simple form of the relation between σ^2 and $\log k_1$ as follows,

$$(a^2/\sigma^2)^2 = K(\log A - \log k_1), \quad (7)$$

where K is an arbitrary constant at a given temperature. In Fig. 2 are plotted the $(r^2/\sigma^2)^2$ values for solution against $\log k_1$. In this figure, we use the nearest neighbor distance r obtained from the present EXAFS analysis in place of the lattice constant a . The straight line in Fig. 2 corresponds to 0.11 of the parameter K and 10.0 of $\log A$. The parameter K is a meaningless arbitrary parameter in the present analysis. While the parameter A is an important parameter indicating a maximum value of the ligand exchange reaction rate pertaining to the zero activation energy or the σ^2 values of infinity. It is remarkable that the value of A coincides with the diffusion-controlled rate in water (order of 10^{10} s^{-1}), which is the inverse of the residence time of water molecules in the vicinity of the metal complex.

Figure 2 shows the result for Rb^+ , which gives a very large σ^2 value of 0.048 \AA^2 . Because of its large σ^2 , the multielectron excitation structure (MEES) observed in the EXAFS signal which is similar to that of Br^- ion in solution.¹⁹⁾ The large σ^2 value is consistent with its fast ligand exchange reaction in aqueous solution ($k_1 = 10^{9.1} \text{ s}^{-1}$). The $(r^2/\sigma^2)^2$ value for Rb^+ of 0.03 lies well on the line for the transition metal ions.

In the present analysis, to obtain the simple relation between E_a and σ^2 , we assume that α is a constant irrespective of the metal ions and σ^2 depends only on D at a given temperature. However, the present EXAFS result appears to suggest that $\log k_1$ depends on $\alpha^2 D$ rather than D since $(r^2/\sigma^2)^2$ linearly depends upon k_1 , as shown in Fig. 2, and $(r^2/\sigma^2)^2$ is theoretically predicted to be proportional to $\alpha^2 D$ from Eq. 4. If the ligand water molecules pass over the potential barrier at infinite distance, E_a could be regarded as being equal to D . However, if the ligand water molecules are exchanged with solvent water at a certain distance from the central metal ion, E_a should depend not only on D but also on

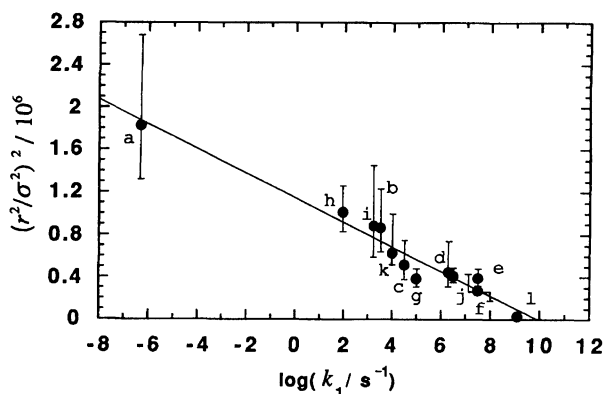


Fig. 2. Relation between $(r^2/\sigma^2)^2$ and $\log k_1$ for solution. The symbols from (a) to (k) are the same as in Fig. 1 and (l) is the result of Rb^+ in aqueous solution. The straight line represents the result of the least squares fitting of Eq. 7 to the experimental data.

α , which is a measure of the force constant for the M–O bond. This interpretation supports the present EXAFS result. Detailed treatment using both α and D is now on progress and will be given in a future work.

Temperature Dependences of σ^2 and C_3 . The EXAFS Debye–Waller factor can be expressed in terms of the dynamical and static contributions. Its temperature dependence gives information about the dynamical contribution. In this section, we briefly mention the relation between the ligand exchange rate constant and the temperature dependences of σ^2 and C_3 .

As shown in Fig. 3, σ^2 is proportional to T in the high temperature region and is constant in the low temperature region, as expected theoretically.¹²⁾ It is found that the higher the ligand exchange rate, the larger the σ^2 and the more rapidly the σ^2 increases with temperature.

The third order cumulant C_3 in the EXAFS reveals the asymmetrical distribution and the anharmonic potential.⁸⁾ It has been apparent theoretically that the temperature dependence of C_3 contains the information regarding the anharmonic potential.¹²⁾ Figure 4 shows the temperature dependences of ΔC_3 , which is defined as the relative value of C_3 at a given temperature T , referred to that at 20 K, i.e. $\Delta C_3 = C_3(T) - C_3(20 \text{ K})$. It is found from the figure that the greater the k_1 value,

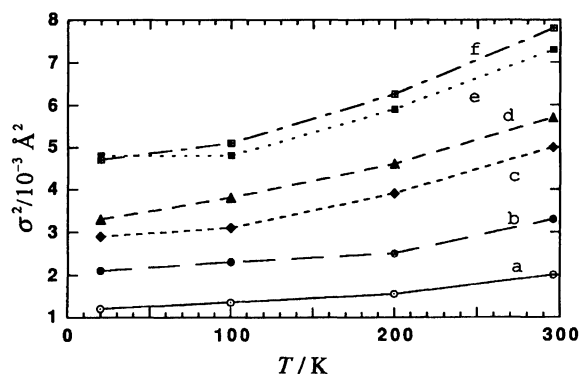


Fig. 3. Temperature dependences of σ^2 for solid hydrated complexes for (a) Cr^{3+} , (b) Fe^{3+} , (c) Ni^{2+} , (d) Co^{2+} , (e) Mn^{2+} , and (f) Zn^{2+} .

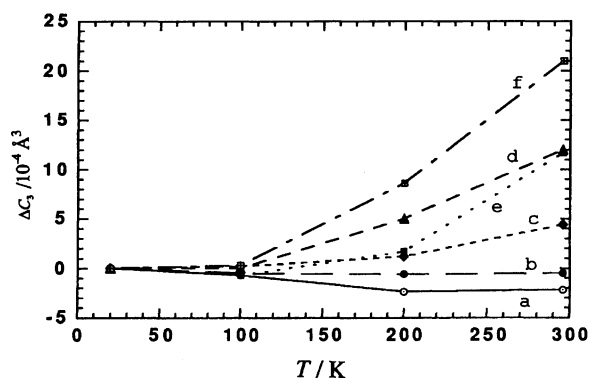


Fig. 4. Temperature dependences of ΔC_3 . The symbols in the figure are the same as in Fig. 3.

the greater the increase in C_3 with temperature, and that C_3 is proportional to T^2 in the high temperature region which has been pointed out in the framework of classical approximation by several authors.^{9–12} While C_3 is constant at low temperature region, which is due to the quantum effect (zero point vibration).¹² It is noted that metal complexes with a greater k_1 value have greater anharmonicity in the potential of metal–oxygen interaction.

The ΔC_3 values for Cr^{3+} and Fe^{3+} do not depend on temperature even in the high temperature range indicating that their potentials are almost harmonic or their vibrational states are not so extensively excited that the anharmonicity does not appear. The temperature dependences of ΔC_3 's for Cr^{3+} and Fe^{3+} are similar, although they have quite different k_1 values in aqueous solution. The reason why the correlation between ΔC_3 and k_1 is poor for Cr^{3+} and Fe^{3+} is because the values of ΔC_3 are obtained from the crystal samples. For the trivalent metal ions, the second-shell water molecules effectively interact with the central metal ion in aqueous solution²⁰ and the structure of the second-shell for solution differs from that for crystal. To reveal the anharmonic potential effect in those complexes, a temperature dependent EXAFS study for the aqueous solution would be useful.

Concluding Remarks

We have found an interesting correlation between the EXAFS Debye–Waller factor and the ligand exchange rate constant for metal ions in solution. A simple expression connecting them was derived by combining the Arrhenius equation and the theory for the EXAFS Debye–Waller factor derived for the Morse type interaction potential. The expression was found to be consistent with the experimental results. The value of the frequency factor A , which corresponds to the maximum limit for the ligand exchange reaction rate, was found to coincide with that of diffusion-controlled reaction.

However, the present analysis contains the following problems:

(1) The Morse potential is employed as the interatomic potential which determines the reaction coordinate for the water exchange reaction in aqueous solution, and the activation energy is assumed to be equal to D . This implies that only the dissociative exchange mechanism is taken into account.

(2) It is assumed that the parameter α does not depend on the kind of metal ion. Judging from the fact that the correlation of Eq. 7 theoretically predicted is experimentally observed in spite of the above two assumptions, these two seem to be closely related to each other. Although the theoretical treatment is limited to σ^2 in this paper, C_3 contains direct information about anharmonicity of the potential. The analysis of the temperature dependence of C_3 should provide the parameters α and D individually. Thus the analysis of C_3 is an

interesting future work concerning the relation between chemical reactivity and the Debye–Waller factor.

(3) Finally, we use the harmonic expression for σ^2 derived by the perturbative method. In this approximation, the displacement of ligand water molecule is supposed to be small. In the real reaction, however, the ligand water molecule must pass over the potential barrier at a more distant position from the central ion. For a more accurate description of the relation between the Debye–Waller factor and the ligand exchange reaction, a non-perturbative technique may be necessary. Then, the Debye–Waller factor of EXAFS would become a useful indicator for the ligand exchange reaction rate in solution.

One of the authors (T. M.) is grateful to Professor T. Fujikawa for helpful discussions and for the financial support from Tosoh corporation. This work has been performed under the approval of the Photon Factory Advisory Committee (proposal no. 90-G034).

References

- 1) H. Ohtaki and T. Radnai, *Chem. Rev.*, **93**, 1157 (1993).
- 2) P. P. Lottici, *Phys. Rev. B*, **35**, 1236 (1987).
- 3) B. S. Brunschwig, C. Crents, D. H. Macartney, T. K. Sham, and N. Sutin, *Faraday Discuss. Chem. Soc.*, **74**, 113 (1974).
- 4) T. K. Sham, *Acc. Chem. Res.*, **19**, 99 (1986).
- 5) T. K. Sham, *Top. Curr. Chem.*, **145**, 81 (1988).
- 6) T. Miyanaga, I. Watanabe, and S. Ikeda, *Chem. Lett.*, **1988**, 1073.
- 7) T. Miyanaga, H. Sakane, I. Watanabe, and S. Ikeda, *Jpn. J. Appl. Phys.*, **32-2**, suppl. 806 (1993).
- 8) E. D. Crozier, J. J. Rehr, and R. Ingalls, "X-Ray Absorption: Principles, Applications, Techniques of EXAFS, SEXAFS and XANES," ed by D. C. Koningsberger and R. Prins, John Wiley, New York (1988), p. 373.
- 9) J. M. Tranquada and R. Ingalls, *Phys. Rev. B*, **28**, 3520 (1983).
- 10) E. A. Stern, P. Livins, and Z. Zhang, *Phys. Rev. B*, **43**, 8850 (1991).
- 11) T. Fujikawa and T. Miyanaga, *J. Phys. Soc. Jpn.*, **62**, 4108 (1993).
- 12) T. Miyanaga and T. Fujikawa, *J. Phys. Soc. Jpn.*, **63**, 1036 (1994).
- 13) H. Sakane, Dr. Thesis, Osaka University, Japan, 1991; H. Sakane, T. Miyanaga, I. Watanabe, N. Matsubayashi, S. Ikeda, and Y. Yokoyama, *Jpn. J. Appl. Phys.*, **32**, 4641 (1993).
- 14) A. G. Mckale, B. W. Veal, A. P. Paulikas, S. K. Chau, and G. S. Knapp, *J. Am. Chem. Soc.*, **110**, 3763 (1988).
- 15) B-K. Teo, "EXAFS: Basic Principles and Data Analysis," Springer-Verlag, New York (1986).
- 16) F. W. Lytle, D. E. Sayers, and E. A. Stern, *Physica B* (Amsterdam), **158**, 701 (1989). (Eq. 2 is used with standard deviation at each point set to 1)
- 17) J. Burgess, "Metal Ions in Solution," Ellis Horwood Ltd., Chichester, England (1978).

- 18) T. J. Swift and R. E. Connick, *J. Chem. Phys.*, **37**, 307 (1962).
19) H. Tanida, H. Sakane, I. Watanabe, and Y. Yokoyama, *Chem. Lett.*, **1993**, 1647.
20) P.-A. Bergstrom and J. Lindgren, *Inorg. Chem.*, **31**, 1529 (1992).
-